Model approximation for the control of large-scale LTI models with guaranteed stability

Pierre Vuillemin, Charles Poussot-Vassal & Daniel Alazard

***Abstract*— Various efficient methods exist for the control of LTI models. Yet these methods can quickly become intractable as the dimension of the considered model increases. Here, a process is described to design a stabilising controller for a large-scale model using model approximation and the robust control framework. The approach is illustrated through the design of an input disturbance rejection control law for the large-scale LTI model representing a flexible space structure.**

I. Introduction

A. Context & motivations

The increasing complexity of some physical systems and the increasing use of numerical tools to model their dynamic behaviour tend to result in *complex models*. In the case of Linear Time Invariant (LTI) models, this complexity translates into a *large dimension* of the state vector. If this dimension is not an issue in theory, it can become a problem in practice. Indeed, the limited computational power of computers and their limited storage capabilities might prevent some control or analysis tools to be used. In addition, the errors induced by floatting point arithmetic might significantly disturb some theoretical results. To alleviate this numerical burden, *model approximation* can be used.

It consists in replacing the initial complex (large-scale) model by a simpler (small-scale) one such that the latter preserves the characteristic properties of the former and remains representative of the underlying physical system it is meant to represent.

Various methods have been developped for the approximation of large-scale models (see [1] for an overview). Some well known methods are the Balanced Truncation [11] and the optimal Hankel approximation [5]. The optimal $\mathcal{H}_2$ model approximation problem has also been widely studied [4], [16], [6] and some efficient algorithms are now available to address it [10], [6]. More recently, the optimal approximation problem in terms of the frequency-limited $\mathcal{H}_2$-norm has been addressed in [13], [19].

In general, the goal of optimal model approximation methods is to minimise the error between the open-loop large-scale and reduced-order models. Therefore, those approaches do not enable to conclude on the error in closed-loop and does not offer any guarantee that a controller synthesised on the low-order model will actually stabilise or achieve some performance on the large-scale model. In this article, model approximation is coupled with the robust control framework to enable to design a stabilising controller for large-scale models.

B. General problem formulation & contributions

The objective of this paper is to demonstrate a generic process that can be used to address the control of large-scale models. This process consists in three steps

(i) first, the large-scale model is approximated using a frequency-limited model approximation method,

(ii) then, a frequency template is built to upper bound the approximation error for all pulsations $\omega \in \mathbb{R}_+$,

(iii) finally, a robust controller is synthesised on the reduced-order uncertain model formed by the reduced-order model obtained at the step *(i)* and the template of the approximation error built at step *(ii)* which is considered as an uncertainty.

This process is illustrated here on a fictitious control problem aimed at designing a control-law performing input disturbance rejection on a large-scale model. The considered model is the International Space Station (ISS) one available in $COMPl_eib$ [8] which represents the transfer of a large flexible space structure with collocated actuators and rate sensors. This model has $n = 270$ states, $n_u = 3$ inputs and $n_y = 3$ outputs.

Note that even if the control problem is not a real application and has been built up, the specifications of the controller have been chosen to be as representative as possible of what could be found in a real applications. Moreover, the proposed approach is not specific to this application and can easily be applied to other control problems.

Besides, the tools used in steps *(i)* and *(ii)* are a part of the MORE Toolbox [14] available at `w3.onera.fr/more/` together with a Matlab® script which enables to reproduce the results presented in this paper.

C. Paper structure

The large-scale control problem is described in Section II and an attempt at addressing it directly through a non-smooth $\mathcal{H}_\infty$ synthesis is presented. Then, in Section III, the large-scale model is approximated and a frequency template is built on the approximation error. In Section IV-B, the small-scale control problem is formulated and addressed with a non-smooth $\mathcal{H}_\infty$-synthesis technique. Finally, Section V concludes this paper and outline some possible outlook for this study.

II. Construction of the control problem

In this section, the control problem used to illustrate the proposed control approach is constructed. In particular, in Section II-A, the initial input disturbance rejection problem

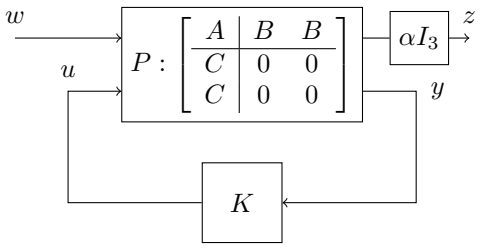

Fig. 1. $\mathcal{F}_l(P,K)$ – General control problem for the input disturbance rejection.

is formulated. It is then completed in Sections II-B and II-C by adding a dynamic to the actuators and a roll-off filter specification on the controller, respectively.

A. Initial control problem

Let $\mathbf{H} := (A,B,C)$ be the state-space realisation of the ISS model and $H(s)$ its associated 3×3 transfer function. The initial control objective is to design a controller K of order $n_k \ll n$ that performs an input disturbance rejection of $x_{dB} = 30$ dB. In other words, one would like to find the controller K such that the difference between the $\mathcal{H}_\infty$-norms of the open and closed loops is, at least, of x_{dB}, *i.e.*

$$20log_{10}\left(\|H\|_{\mathcal{H}_\infty}\right) - 20log_{10}\left(\|H_{BF}\|_{\mathcal{H}_\infty}\right) \geq x_{dB},$$

which can be rewritten as

$$\|H_{BF}\|_{\mathcal{H}_\infty} \leq 10^{-x_{dB}/20}\|H\|_{\mathcal{H}_\infty} = \frac{1}{\alpha}, \qquad (1)$$

where $\alpha = 272.88$ here. This disturbance rejection problem can be formulated as a standard $\mathcal{H}_\infty$ control problem aimed at finding K which solves the non-smooth optimisation problem,

$$K = \arg \min_{\substack{\text{stabilising } \tilde{K} \\ \tilde{K}\in\mathcal{K}}} \|\mathcal{F}_l(P,\tilde{K})\|_{\mathcal{H}_\infty},$$

where $\mathcal{F}_l(P,K)$ is the lower Linear Fractional Representation (LFR)[1] formed by interconnecting the plant P with the gain K as represented in Figure 1 and $\mathcal{K}$ represents the set of n_k-th order rational transfer matrices.

Note that the $\mathcal{H}_\infty$-norm of the LFR $\mathcal{F}_l(P,K)$ is simply the $\mathcal{H}_\infty$-norm of the closed-loop H_{BF} from (1) scaled by α,

$$\|H_{BF}\|_{\mathcal{H}_\infty} = \frac{1}{\alpha}\|\mathcal{F}_l(P,K)\|_{\mathcal{H}_\infty}$$

hence the disturbance rejection specification (1) can be rewritten as

$$\|\mathcal{F}_l(P,K)\|_{\mathcal{H}_\infty} \leq 1. \qquad (2)$$

Since the model $\mathbf{H}$ is positive, finding a controller K satisfying the rejection specification (2) is simple (see for instance [3]). Any sufficiently large negative static feedback enables to damp all frequencies. Indeed, $\mathcal{F}_l(P,K) = \alpha(I_3 - KH)^{-1}$, then if the magnitude of KH is large enough with respect to 1, one can approximate the lower LFR $\mathcal{F}_l(P,K)$ as

$$\mathcal{F}_l(P,K) \approx -\alpha K^{-1}. \qquad (3)$$

The approximation (3) suggests that for satisfying the disturbance rejection constraint (2), the static gain $K_1 = -\alpha I_3$ can be used. And indeed, one can check that the $\mathcal{H}_\infty$-norm of the lower LFR $\mathcal{F}_l(P,K_1)$ satisfies inequality (2),

$$\|\mathcal{F}_l(P,K_1)\|_{\mathcal{H}_\infty} = 0.9693 < 1.$$

This is illustrated in Figure 2 where the singular values of the open-loop and closed-loop models $\mathbf{H}$ and $\mathcal{F}_l(P,K_1)$ are plotted.

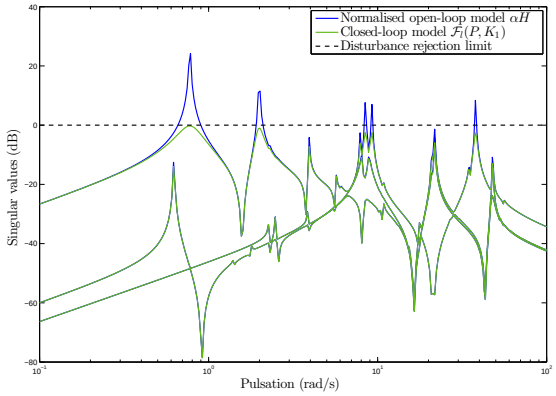

Fig. 2. Singular values of the open-loop model $\mathbf{H}$ and of the closed-loop model $\mathcal{F}_l(P,K_1)$ obtained with the static output feedback K_1.

B. Adding the actuators

To make the control problem more interesting and more realistic, a dynamic is added to represent the actuators. Let us consider the actuator $A_c(s) = a_c(s)I_3$ where $a_c(s)$ is a damped second-order low-pass filter of bandwidth 20 rad/s, *i.e.*

$$a_c(s) = \frac{\omega_a^2}{s^2 + \xi_a\omega_a s + \omega_a^2},$$

with $\xi_a = 1.4$ and $\omega_a = 20$rad/s. Note that the actuator is built to have a static gain of 1, which means that the assumption is made that it does not disturb the low frequency and does not modify the $\mathcal{H}_\infty$-norm of the LFR.

The $\mathcal{H}_\infty$ control problem is consequently modified and consists now in finding the controller K which solves

$$K = \arg \min_{\substack{\text{stabilising } \tilde{K} \\ \tilde{K}\in\mathcal{K}}} \|\mathcal{F}_l^{(2)}(P,\tilde{K})\|_{\mathcal{H}_\infty}, \qquad (4)$$

where $\mathcal{F}_l^{(2)}(P,K)$ is the LFR obtained by adding the actuator dynamics to $\mathcal{F}_l(P,K)$ as represented in Figure 3.

One can easily checks that the former static output feedback K_1 is no longer sufficient when the actuators dynamic is taken into account, indeed

$$\|\mathcal{F}_l^{(2)}(P,K_1)\|_{\mathcal{H}_\infty} = 6.5079 > 1.$$

[1] A very comprehensive description of the LFR and associated manipulation can be found in [9].

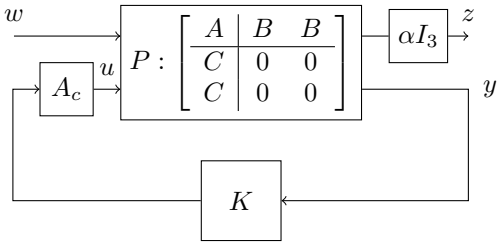

Fig. 3. $\mathcal{F}_l^{(2)}(P,K)$ – General control problem for the input disturbance rejection with the actuator dynamic.

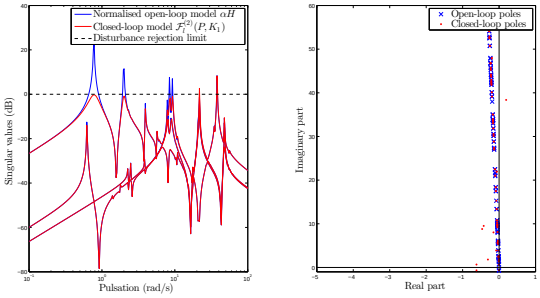

Fig. 4. Singular values of the open-loop and closed-loop models $\mathbf{H}$ and $\mathcal{F}_l^{(2)}(P,K_1)$ (left) and poles of the open-loop and closed-loop models $\mathbf{H}$ and $\mathcal{F}_l^{(2)}(P,K_2)$ where $K_2 = 3K_1$ (right).

This can also be seen in Figure 4 (left) where the singular values of the open-loop and closed-loop models are plotted. More importantly, the closed-loop has poor stability magerins and becomes unstable when the feedback gain increases, for instance one can observe in Figure 4 (right) that the closed-loop $\mathcal{F}_l^{(2)}(P,K_2)$ where $K_2 = 3K_1$ has unstable poles. Hence, a dynamic controller has to be found to fulfil the disturbance rejection when the actuator dynamic is taken into account.

C. Roll-off filter specification

In practice, it is common to restrain the dynamics of a controller in high frequency in order to *(i)* attenuate the transmission of measurement noise and *(ii)* to avoid the local inversion of the actuator in the controller with an optimal $\mathcal{H}_\infty$ synthesis[2]. This constraint can be translated in the $\mathcal{H}_\infty$ control framework by adding the optimisation objective $\|WK\|_{\mathcal{H}_\infty}$, where $W(s)$ is a roll-off filter, to the previous optimisation problem (4) which therefore becomes multiobjective,

$$K = \arg \min_{\substack{\text{stabilising } \tilde{K} \\ \tilde{K} \in \mathcal{K}}} \max\{\|\mathcal{F}_l^{(2)}(P,\tilde{K})\|_{\mathcal{H}_\infty}, \|W\tilde{K}\|_{\mathcal{H}_\infty}\}. \tag{5}$$

If the controller $K(s)$ is such that $\|WK\|_{\mathcal{H}_\infty} \leq 1$, then it means that its dynamics are upper bounded by the inverse of the roll-off filter $W(s)$, *i.e.*

$$\sigma_{max}(K(j\omega)) \leq \sigma_{max}(W^{-1}(j\omega)), \forall \omega \in \mathbb{R},\ i = 1,\ldots,3.$$

In addition, $\|WK\|_{\mathcal{H}_\infty} \leq 1$ ensures the *strong stabilisation*, that is to say that the controller $K(s)$ is stable. This property is quite recommended in space applications from a practical implementation point of view.

Here the roll-off filter $W(s)$ is designed in the following way

- one would like a roll-off of 40dB/decade on each axis, hence the roll-off filter $W(s)$ is chosen as a diagonal transfer matrix where each diagonal entry is a damped, invertible, second-order model.
- In addition, since one knows that α is the required gain to achieve the disturbance rejection specification without actuator (see Section II-A), the controller must, at least, be allowed to reach this value for pulsations lower than $\omega_{ro} = 40$rad/s where the last resonance of the model $\mathbf{H}$ is located. Hence, one wants that

$$\sigma_{max}(W^{-1}(j\omega_{ro})) = \rho\alpha,\ \rho > 1,$$

Here, ρ is set to 3 in order not to be too restrictive.

By taking into account these two points, the filter can be chosen for instance as

$$W(s) = \frac{1}{\rho\alpha} \frac{\frac{s^2}{\omega_{ro}^2}}{\frac{1}{(p\omega_{ro})^2}s^2 + \frac{\xi}{p\omega_{ro}}s + 1} I_3,$$

where $\rho = 3$, $\omega_{ro} = 40$ rad/s, $p = 300$, $\xi = 1.4$. Note that decreasing ρ or ω_{ro} makes the control problem harder since the inverse of $W(s)$ is then constraining the dynamics of the controller directly below 40rad/s where the last resonance of the model is located.

Since the filter $W(s)$ imposes a second-order roll-off on each one of the three axis, the order of the controller must at least be equal to 6. Hence in the sequel, the order of the controller $K(s)$ is set to $n_k = 6$.

D. Solving the large-scale $\mathcal{H}_\infty$ control problem

The multiobjective $\mathcal{H}_\infty$ control problem (5) can be solved using dedicated non-smooth optimisation tools [2], [7]. However, the size of the model $\mathbf{H}$ slows down the optimisation process and can prevent it from satisfying the constraints due to the presence of more local minima.

Here, the routine included in Matlab® is used to address (5) :

- without any restart, no satisfactory controller is found, indeed $\gamma = 2.8$ (the synthesis takes $\sim$ 5min on a standard computer),
- by adding some restarts, a controller solving (5) can be found but the design is quite slow in that case ($\sim$ 40 min with 2 restarts[3]).

One can see that the large-scale control problem can be solved directly using restarts. Yet given the dimension of the

[2]Indeed, $K(s) = -\alpha A_c^{-1}(s)$ cancels the dynamics of the actuator and achieves the disturbance rejection. Yet in practice, it is not acceptable because the dynamic of the actuator is not perfectly known and noise is likely to be present on the output y.

[3]The required computation times greatly varies depending on the number of iterations.

problem, the design is slow and the use of random restarts is not fully satisfactory since the results cannot be reproduced. Model approximation can be used to simplify the design process.

III. Approximation of the large-scale model

In this section, the construction of the models used to build the small-scale control problem is described. In particular, the large-scale model is reduced in Section III-A and a frequency template embedding the approximation error is built in Section III-B.

A. Frequency-limited model approximation

Description of the considered model approximation method. The model approximation method considered here is called *Descent Algorithm for Residues and Poles Optimisation* (**DARPO**) and has been proposed in [19]. Its principle is briefly recalled thereafter.

Given a n-th order large-scale model $\mathbf{H}$ and a frequency interval Ω, **DARPO** finds a reduced-order model $\hat{\mathbf{H}}$ of order $r \ll n$ which solves the *optimal* $\mathcal{H}_{2,\Omega}$ *approximation problem*, *i.e.*

$$\hat{H} = \arg \min_{rank(G)=r} \|H - G\|^2_{\mathcal{H}_{2,\Omega}}, \tag{6}$$

where the $\mathcal{H}_{2,\Omega}$-norm is defined as the restriction of the $\mathcal{H}_2$-norm over Ω, *i.e.*

$$\|H\|^2_{\mathcal{H}_{2,\Omega}} := \frac{1}{\pi} \int_{\Omega} \|H(j\nu)\|^2_F \, d\nu.$$

To solve (6), **DARPO** relies on the poles-residues formulation of the $\mathcal{H}_{2,\Omega}$-norm [18] and finds the poles and associated residues of the reduced-order model which satisfy the first-order optimality conditions associated to (6). More specifically, the method uses an unconstrained quasi-Newton optimisation scheme (see for instance [12]) based on the BFGS update for complex variables [15].

Note that the model approximation problem (6) is both non-linear and non-convex. Since **DARPO** relies on a local optimisation algorithm, the reduced-order model obtained is a local minimum of problem (6).

Approximation of the ISS model. Here, the ISS model $\mathbf{H}$ is approximated to an order 30 over the frequency interval $\Omega = [0, 40]$.

The singular values of the large-scale model $\mathbf{H}$ and the reduced-order one $\hat{\mathbf{H}}$ are plotted in Figure 5. One can observe that almost all the dynamics of the large-scale model are reproduced by the reduced-order one.

B. Construction of a frequency template of the approximation error

The objective here is to build a frequency template $\mathbf{G}$ which transfer matrix $G(s)$ satisfies, for $\omega \in \mathbb{R}_+$,

$$\sigma_{max}(G(j\omega)) \geq \sigma_{max}(H(j\omega) - \hat{H}(j\omega)). \tag{7}$$

Indeed, with such a frequency template, the large-scale model $\mathbf{H}$ can be represented as a low-order uncertain model

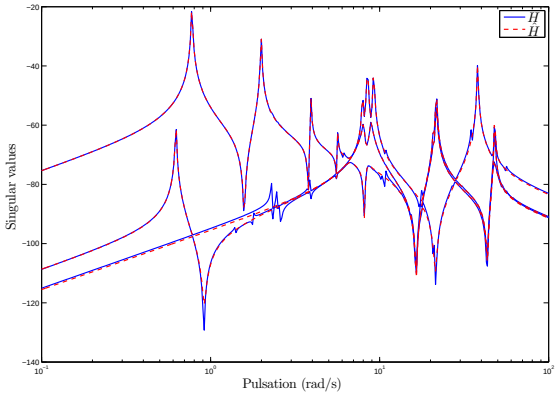

Fig. 5. Singular values of the large-scale model $\mathbf{H}$ and its 30-th order approximation $\hat{\mathbf{H}}$.

represented by $\hat{\mathbf{H}}$ and $\mathbf{G}$. To simplify the determination of the frequency template, two simplifying steps are used :

1) First, instead of the highest singular value in (7), one considers rather the Frobenius norm and looks for $\mathbf{G}$ such that, for $\omega \in \mathbb{R}_+$,

$$\begin{aligned} \sigma_{max}(G(j\omega)) &\geq \left\| H(j\omega) - \hat{H}(j\omega) \right\|_F \\ &\geq \sigma_{max}(H(j\omega) - \hat{H}(j\omega)). \end{aligned} \tag{8}$$

2) If $\mathbf{G}$ is an arbitrary n_G-th order model, determining its parameters such that $G(s)$ satisfies (8) remains a complex problem. It is simplified here by imposing a (restrictive) structure to $G(s)$,

$$G(s) = K \left(\frac{s - z}{s - p} \right)^{n_G}, \tag{9}$$

where $p < z < 0$[4]. With this structure, the constraint (8) can be restricted to

$$\begin{aligned} \sigma_{max}(G(j\omega_k)) &\geq \left\| H(j\omega_k) - \hat{H}(j\omega_k) \right\|_F \\ &\geq \sigma_{max}(H(j\omega_k) - \hat{H}(j\omega_k)), \end{aligned}$$

where the pulsations ω_k are such that

$$\left\| H(j\omega_k) - \hat{H}(j\omega_k) \right\|_F = \max_{\omega \in [0, \omega_k + \epsilon]} \left\| H(j\omega) - \hat{H}(j\omega) \right\|_F. \tag{10}$$

The ω_k are the pulsations where the Frobenius norm of the transfer function dominates its value for lower pulsations.

The relevant pulsations ω_k defined by (10) can be determined by exploiting the results presented in [20] where two bounds on the $\mathcal{H}_\infty$-norm of a LTI model have been derived. In particular, considering a LTI model $\mathbf{L}$, one of the bound, denoted Γ_Ω, is such that

$$\Gamma_\Omega(L) = \max_{\omega \in \Omega} \|L(j\omega)\|_F \geq \max_{\omega \in \Omega} \sigma_{max}(L(j\omega))$$

[4]With $p < z$, the frequency template is tighter in low frequency than in high frequency which is coherent with the fact that the reduction is generally performed so that the low frequency behaviour of the large-scale model is matched.

where Ω is some frequency interval. Hence, by iteratively decreasing the interval of research Ω of the bound Γ_Ω from $[0, \infty)$ to 0, the pulsations satisfying (10) can be found. The approach is summarised in Algorithm 1.

Algorithm 1 Computation of the relevant pulsations ω_k from (10)

Require: A LTI model $\mathbf{H}$

Set $\Omega_0 = [0, \infty)$ and compute $\tau_0 = \Gamma_{\Omega_0}(H)$ with its associated pulsation ω_0 with the method proposed in [20].
$i \leftarrow 1$
while $\omega_{i-1} > \epsilon$ **do**
  Set $\bar{\omega} = \omega_{i-1}$ and $\omega = \omega_{i-1}$
  while $\bar{\omega} = \omega$ **do**
    Set $\omega \leftarrow \omega - \rho$ where $\rho > 0$ and $\Omega = [0, \omega]$
    Compute $\Gamma_\Omega(H)$ and the associated pulsation $\bar{\omega}$
  end while
  Set $\omega_i = \bar{\omega}$ and $\tau_i = \Gamma_\Omega(H)$.
  $i \leftarrow i + 1$
end while

Note that ρ in Algorithm 1 is a tuning parameter which controls the decrease of the interval of research. It must not be too large in order to avoid missing relevant pulsations and it must not bee too small so that the procedure is not too slow.

Then, the frequency template $\mathbf{G}$ is determined in an heuristic and simple way. First, one imposes that the static gain of the frequency template $\mathbf{G}$ is equal to the Frobenius norm of the non-null static gain of the error

$$G(0) = \underbrace{\left\| H(0) - \hat{H}(0) \right\|_F}_{e_0}.$$

This constraint is coherent with the structure of the frequency template which is meant to be tight in low frequency. In addition, for each couple of gain and pole $\{K, p\}$, it enables to determine the zero z of the frequency template as,

$$z = \left(\frac{e_0}{K}\right)^{\frac{1}{n_G}} p. \tag{11}$$

The remaining two parameters K and p are determined by relaxing their value from initial values that violate the constraints (8) until they are all satisfied. The procedure is summarised in Algorithm 2. The way the gain and the pole are relaxed is a tuning parameter that can be adjusted to modify the shape of the template. Similarly, the order n_G of the frequency template can be adjusted to steepen its response.

The second-order frequency template obtained here with the reduced-order model from Section III-A is plotted in Figure 6. One can observe that in this case, the use of the Frobenius norm does not induce too much conservatism in comparison to the highest singular value.

Algorithm 2 Algorithm for the construction of a frequency template

Require: A LTI model $\mathbf{H}$ to be upper bounded, the order n_G of the frequency template.

Compute all the relevant pulsations $\boldsymbol{\omega} \in \mathbb{R}^K$ an associated gains $\boldsymbol{\tau} \in \mathbb{R}^K$ with Algorithm 1.
Set $p_1 = -\max_j(\boldsymbol{\omega}_j)$ and $K_1 = \max_j(\boldsymbol{\tau}_j)$.
Compute z_1 as in equation (11).
Build G_1 as in equation (9).
$i = 1$.
while the constraints (8) are not satisfied **do**
  $p_{i+1} \leftarrow -\alpha |p_i|$ with $0 < \alpha < 1$.
  $K_{i+1} \leftarrow \beta K_i$ with $\beta > 1$.
  Update the zero z_{i+1} as in equation (11) with p_{i+1} and K_{i+1}.
  Build $G_{i+1}(s)$ as in equation (9).
  $i \leftarrow i + 1$.
end while
return The frequency template $\mathbf{G}$.

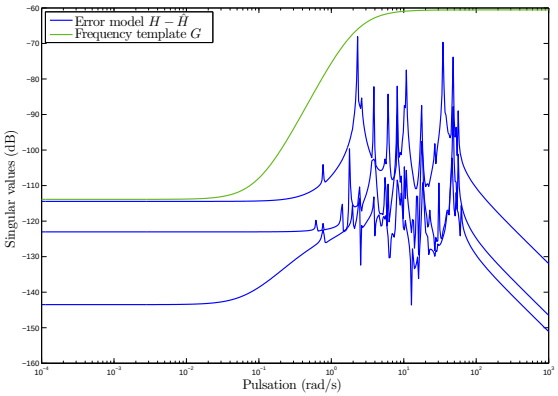

Fig. 6. Singular values of the approximation error $\mathbf{H} - \hat{\mathbf{H}}$ and of the corresponding frequency template $\mathbf{G}$.

IV. Small-scale control problem

In this section, the reduced-order model $\hat{\mathbf{H}} = (\hat{A}, \hat{B}, \hat{C})$ and the frequency template $\mathbf{G}$ are used to build a small-scale control problem almost equivalent to the one presented in Section II. Firstly, in Section IV-A, the control problem that must be solved to ensure the stability of the large-scale plant is presented. In Section IV-B, the final small-scale control problem is described and it is solved in Section IV-C.

A. Stabilising the large-scale plant

By synthesising a controller $K(s)$ that ensures the *robust stability* of $\hat{\mathbf{H}}$ with respect to the uncertainty $\mathbf{G}$, then it is guaranteed to stabilise the large-scale model $\mathbf{H}$. Hence, a stabilising controller $K(s)$ for $\mathbf{H}$ can be found by solving the following $\mathcal{H}_\infty$ control problem

$$K = \arg \min_{\substack{\text{stabilising } \tilde{K} \\ \tilde{K} \in \mathcal{K}}} \|\mathcal{F}_l^{(3)}(\hat{P}, \tilde{K})\|_{\mathcal{H}_\infty},$$

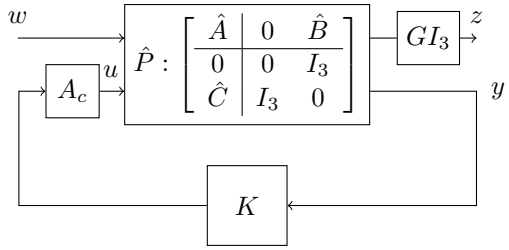

Fig. 7. Lower LFR $\mathcal{F}_l^{(3)}(\hat{P}, K)$ for the robust stability with respect to the uncertainty G representing the approximation error.

where $\mathcal{F}_l^3(\hat{P}, K)$ is the low-order LFR formed by interconnecting the reduced-order plant $\hat{P}$ with $K(s)$ and $A_c(s)$ and by adding the uncertainty $G(s)$ in output of the performance channel as represented in Figure 7.

Note that the method proposed in Section III-B to build the frequency template $\mathbf{G}$ produces a SISO model while the plant here is MIMO. That is why one has to create the MIMO transfer matrix $G(s)I_3$.

B. Final alternative small-scale control problem

Finally, one can formulate a small-scale $\mathcal{H}_\infty$ control problem which is similar to the original large-scale problem presented in Section II. In particular, instead of (5), one rather wants to find $K(s)$ that solves

$$K = \min_{\substack{\text{stabilising } \tilde{K} \\ \tilde{K} \in \mathcal{K}}} \max\{\|\mathcal{F}_l^{(2)}(\hat{P}, \tilde{K})\|_{\mathcal{H}_\infty}, \|W\tilde{K}\|_{\mathcal{H}_\infty}, \ldots \|\mathcal{F}_l^{(3)}(\hat{P}, \tilde{K})\|_{\mathcal{H}_\infty}\}. \quad (12)$$

The differences between the $\mathcal{H}_\infty$ control problem (5) and (12) are

(i) the new $\mathcal{H}_\infty$ problem involves only low-order models while the problem (5) involves the initial large-scale plant P,

(ii) the optimisation channel $\|\mathcal{F}_l^{(3)}(\hat{P}, \tilde{K})\|_{\mathcal{H}_\infty}$ in (12) ensures that the controller $K(s)$ stabilises the *large-scale* plant P by synthesising a robust controller on the low-order uncertain model (see Section IV-A),

(iii) the performance channel $\|\mathcal{F}_l^{(2)}(\hat{P}, \tilde{K})\|_{\mathcal{H}_\infty}$ guarantees that the controller $K(s)$ ensures the disturbance rejection *on the low-order LFR* $\mathcal{F}_l^{(2)}(\hat{P}, \tilde{K})$ but it is not necessarily true on the large-scale one $\mathcal{F}_l^{(2)}(P, \tilde{K})$.

The last point implies that the $\mathcal{H}_\infty$-norm of $\mathcal{F}_l^{(2)}(P, \tilde{K})$ must be recomputed afterwards to check if it is inferior to 1 (see Remark 1). With a sufficiently accurate reduced-order model $\hat{\mathbf{H}}$, one expects the constraint to be satisfied though.

Remark 1 (Robust performance): In order to guarantee that the disturbance rejection is satisfied on the large-scale model, the controller $K(s)$ should be synthesised using μ-synthesis to ensure the *robust performance* of the controller with respect to the approximation error.

The available methods for μ-synthesis lead to controllers of the same dimension as the plant which is not necessarily interesting. One way to address the issue here is to perform a $\mathcal{H}_\infty$ synthesis based on the $\mathcal{H}_\infty$ control problem represented in Figure 8. This standard problem $M(s)$ involves static scaling $\frac{1}{\alpha}$ and α to normalise the direct feedthrough from w_1 to z_2 to 1. Then a sufficient (but not necessary) condition for robust performance consists in finding a stabilising controller K such that $\|\mathcal{F}_l(M, K)\|_{\mathcal{H}_\infty} \leq 1$. Since this condition is only sufficient, the controller might be conservative.

However here, with the specifications considered in the control problem, no satisfactory solution is found with this approach.

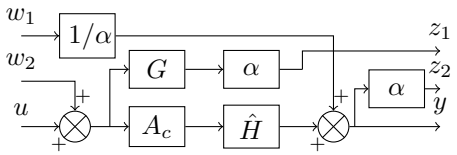

Fig. 8. Plant $M(s)$ representing the sufficient $\mathcal{H}_\infty$ control problem for robust performance.

C. Solving the small-scale control problem

A satisfactory controller $K(s)$ for the small-scale control problem (12) is found without any restart (see Remark 2 for some comments about the computation time) such that

$$\max\{\|\mathcal{F}_l^{(2)}(\hat{P}, K)\|_{\mathcal{H}_\infty}, \|WK\|_{\mathcal{H}_\infty}, \|\mathcal{F}_l^{(3)}(\hat{P}, K)\|_{\mathcal{H}_\infty}\} = 0.9086 < 1,$$

which means that the robust stability, the roll-off specification and the disturbance rejection on the low-order plant are all satisfied. To verify that the disturbance rejection is also satisfied on the large plant P, one must compute the $\mathcal{H}_\infty$-norm of the large LFR, *i.e.*

$$\|\mathcal{F}_l^{(2)}(P, K)\|_{\mathcal{H}_\infty} = 0.9097 < 1.$$

The disturbance rejection of 30dB can be seen in Figure 9 where the singular values of the open-loop, low-order closed-loop and large-scale closed-loop are plotted. The difference between the low-order (green) and the large-scale (red) closed-loops is barely noticeable here. One can also see that the synthesised controller $K(s)$ satisfies the constraint imposed by the roll-off filter $W(s)$ in Figure 10.

Remark 2: (Time required to build and solve the small-scale control problem) Reducing the large-scale model $\mathbf{H}$ with **DARPO** to an order 30 takes $\sim$ 3s, building the frequency template requires $\sim$ 1.4s and synthesising the controller $K(s)$ takes $\sim$ 58s (with 287 iterations). Hence, the small-scale control problem is built and addressed in about one minute. Obviously, the guarantees are not the same than with the large-scale control problem (5), but solving the small-scale problem is significantly faster.

About the choice of the model approximation method. In Section III-A, the large-scale model is reduced over a bounded frequency interval with **DARPO**. The same process can be performed with another frequency interval and other model approximation methods. Yet here, the other settings that have been considered did not lead to a satisfactory

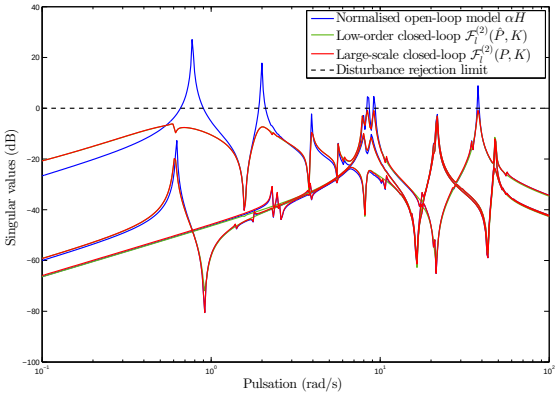

Fig. 9. Singular values of the normalised open-loop model $\mathbf{H}$, of the low-order closed loop $\mathcal{F}_l^{(2)}(\hat{P},K)$ and of the large-scale closed-loop $\mathcal{F}_l^{(2)}(P,K)$.

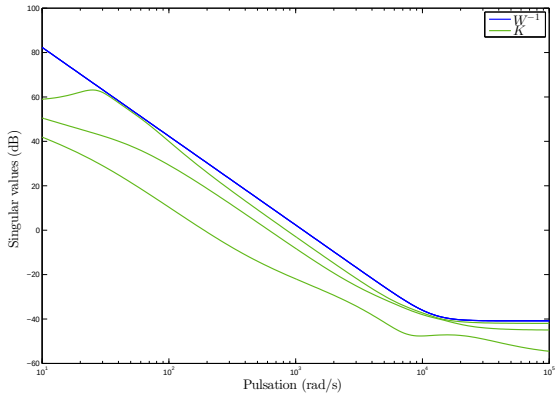

Fig. 10. Singular values of the 6-th order controller $K(s)$ synthesised on problem (12) and of the inverse of the roll-off filter $W^{-1}(s)$.

controller. In Table I, the value of γ obtained by considering other model approximation settings are reported.

It is likely that **DARPO** considered over $\Omega = [0, 40]$ catches a dynamic that the other methods miss and which is important in closed-loop. Yet determining a priori which are the relevant dynamics for the closed-loop is not a trivial task.

V. Conclusion

In this paper, the control of a large-scale LTI model is addressed by coupling model approximation and the robust control framework. In particular, the large-scale model is reduced and the approximation error induced by this step is modelled by a low complexity frequency template which is then considered as an uncertainty. A controller robust to this uncertainty is then synthesised on the low-order model which guarantees that the controller also stabilises the large-scale plant. This process has been illustrated on a non-trivial disturbance rejection problem.

The approach can readily be extended to other control problems but some points need still to be clarified. In particular, what model approximation method, reduction order and reduction interval are adequate for a given control problem is not obvious to determine and this question is still under investigation.

In addition, the proposed method for building a frequency template can be improved by complexifying the structure of the template so that it is less conservative. A simple extension has for instance been considered in [17] by using two filters in serie with the same simple structure as the one used here.

Approximation method	γ
DARPO $\Omega = [0, 40]$	0.91
DARPO $\Omega = [0, \infty)$	1.14
Balanced Truncation	1.28
Hankel norm approximation	1.14

TABLE I

Final objective function γ of the control problem (12) for different model approximation methods.

References

[1] A.C. Antoulas. *Approximation of large-scale dynamical systems*. SIAM, 2005.

[2] P. Apkarian and D. Noll. Nonsmooth $\mathcal{H}_\infty$ synthesis. *IEE Transactions on Automatic Control*, 51(1):71 – 86, 2006.

[3] A.V. Balakrishnan. Robust stabilizing compensators for flexible structures with collocated controls. *Applied Mathematics and Optimization*, 33(1):35 – 60, 1996.

[4] L. Baratchart, M. Cardelli, and M. Olivi. Identification and rational $\mathcal{L}_2$ approximation : A gradient algorithm. *Automatica*, 27(2):413 – 417, 1991.

[5] K. Glover. All optimal Hankel-norm approximations of linear multivariable systems and their $\mathcal{L}_\infty$-error bounds. *International Journal of Control*, 39(6):1115 – 1193, 1984.

[6] S. Gugercin, A.C. Antoulas, and C. Beattie. $\mathcal{H}_2$ model reduction for large-scale linear dynamical systems. *SIAM Journal on Matrix Analysis and Applications*, 30(2):609 – 638, 2008.

[7] S. Gumussoy, D. Henrion, M. Millstone, and M.L. Overton. Multiobjective robust control with HIFOO 2.0. In *Proceedings of the 6th IFAC symposium on robust control design*, 2009.

[8] F. Leibfritz and W. Lipinski. Description of the benchmark examples in *COMPl$_e$ib* 1.0. Technical report, University of Trier, 2003.

[9] J.F. Magni. Linear fractional representation toolbox for use with Matlab. Available at http://w3.onera.fr/smac/, 2006.

[10] J-P. Marmorat, M. Olivi, B. Hanzon, and R.L.M. Peeters. Matrix rational $\mathcal{H}_2$ approximation: A state-space approach using Schur parameters. In *Proceedings of the Conference on Decision and Control*, volume 4, pages 4244 – 4249, 2002.

[11] B. Moore. Principal component analysis in linear systems: controllability, observability, and model reduction. *IEEE Transactions on Automatic Control*, 26(1):17 – 32, 1981.

[12] J. Nocedal and S.J. Wright. *Numerical optimization*. Springer, 1999.

[13] D. Petersson and J. Löfberg. Model reduction using a frequency-limited $\mathcal{H}_2$-cost. *Systems & Control Letters*, 67(0):32 – 39, 2014.

[14] C. Poussot-Vassal and P. Vuillemin. Introduction to MORE: a MOdel REduction Toolbox. In *Proceedings of the Multi-conference on Systems and Control*, pages 776 – 781, 2012.

[15] L. Sorber, M. Van Barel, and L. De Lathauwer. Unconstrained optimization of real functions in complex variables. *SIAM Journal on Optimization*, 22(3):879 – 898, 2012.

[16] P. Van Dooren, K.A. Gallivan, and P.A. Absil. $\mathcal{H}_2$-optimal model reduction of MIMO systems. *Applied Mathematics Letters*, 21(12):1267 – 1273, 2008.

[17] P. Vuillemin, F. Demourant, J-M. Biannic, and C. Poussot-Vassal. Global stability validation of an uncertain large-scale aircraft model. In *Proceedings of the Multi-conference on Systems and Control*, 2014.

[18] P. Vuillemin, C. Poussot-Vassal, and D. Alazard. A spectral expression for the frequency-limited $\mathcal{H}_2$-norm. Available as arXiv:1211.1858, 2012.

[19] P. Vuillemin, C. Poussot-Vassal, and D. Alazard. Poles residues descent algorithm for optimal frequency-limited $\mathcal{H}_2$ model approximation. In *Proceedings of the European Control Conference*, pages 1080 – 1085, 2014.

[20] P. Vuillemin, C. Poussot-Vassal, and D. Alazard. Two upper bounds on the $\mathcal{H}_\infty$-norm of LTI dynamical systems. In *Proceedings of the IFAC World Congress*, pages 5562 – 5567, 2014.